A Distributed Gaussian Weight Function based Deep Spectral Cluster Learning and Enhanced Deep Patch Level Classifier for Detection of Diabetic Retinopathy

J. Usha Nandhini and Dr.S. Lakshmi Prabha

Abstract---Diabetic retinopathy (DR) is an intimidating of vision menacing, through chronic diabetes mellitus caused by destruction to the retina's blood vessels. Being one of the major prevalent issues of blindness, it is generally affect the adults. Automatic identification of DR lesions may contribute to the screening and diagnosis of this affliction in digital fundus images. The Improved Deep Instance Learning approach, utilized for DR identification in our earlier research activity, that mutually recognizes attributes and classifiers from the results and enables a considerable augmentation in the identification of DR images and their internal lesions. Nevertheless, This Deep Instance Learning process does not refine the concluding threshold, which used to acquire hard labels, in this manner, resulting in poor precision and huge complication in computation as well. To solve this issue, this study suggests the Deep Spectral Cluster Learning (DGW-DSCL) based on Distributed Gaussian Weight strategy to identify diabetic retinopathy in order to make the execution of classifier better. The structural similarity index (SSI) criterion is previously used to assess the purity of image. Through the novel Fuzzy histogram equalization, the augmentation of equalization and variation is achieved. And then the Deep Spectral Cluster Learning (DGW-DSCL) based on Distributed Gaussian Weight strategy is implemented, which streamlines an embedding method through Gaussian weight process such that the observed depictions of comparable entities objects are clustered into the same array and distinct entities included in varying clusters to improve the expertise of the spectral clustering. Then it is suggested to forecast the Diabetic Retinopathy (DR) chances by those integrated data inserted into the advanced classifier of deep patch-level, in which the classifier's weight values are modified, using the Grey Wolf Optimization (IVIR-) algorithm based on Improved Variability Iteration Ratio. The simulation findings reveal that the methodology suggested has an extreme certainty contrast to the current prediction strategies.

Keywords--- Diabetic Retinopathy, Structural Similarity Index (SSI), Fuzzy Histogram Equalization, Distributed Gaussian Weight Function based Deep Spectral Cluster Learning (DGW-DSCL), Deep Neural Network Classifier, Improved Variability Iteration Ratio based Grey Wolf Optimization (IGWO).

I. INTRODUCTION

Diabetic retinopathy (DR) is a debilitating eye condition that arises from diabetes mellitus and has developed to be the exceedingly familiar occurrence of blindness now a days. Based on the recent stats, the international predominance of diabetes [1] had an exponential rise of 4.4 per cent, by 2030. Diabetes retinopathy (DR) is a

J. Usha Nandhini, Research & Development Centre, Bharathiar University, Coimbatore. E-mail: jushanandhini@gmail.com
Dr.S. Lakshmi Prabha, Assistant Professor, Department of Computer Science, Government Arts College for Women, Salem.
E-mail: lpgac2007@gmail.com

pathological circumstance in which the retina is weakened due to fluid infiltration into the retina from the blood vessels. It is one of the very frequent eye disorders with diabetes, and a root cause of visual impairment. Up to 415 million diabetic sufferers are at threat of visual impairment due to diabetics. It takes place as diabetes affects the fairly small blood vessels within the retina, the bright-sensitive tissue behind the eye [2]. Diabetes that causes cataracts, glaucoma and, most notably, damage to the blood vessels within the eye will impair the patient's vision, which is a disorder defined as "diabetic retinopathy." This small blood vessel spills blood and fluid on the retina that creates the causes like hemorrhages, micro-aneurysms, cotton wool patches, rough exudates or venous loops.

There are various sections such as the macula, oculus dextrus (OD), oculus sinister (OS), fovea, in every human eye, that they get an impact on the blood vessels and are less in contrast with the retinal walls. The first element to identify is the blood vessel segmentation that will help in detection[3]. The blood vein walls in the retina have several criteria including diameter, color, weight, length, branches, tortuosity, etc. Multiple eye illnesses have recognizable side effects that direct their illness detection. The DR can also be detected by the segmentation of the OS, OD w.r.t. blood vessels and the separation of nerves / capillaries in the fundus images.Retinal vein impediment describes the symptom of expanded intricateveins, occlusion of Retinal Artery has modified the shades of copper or silver-shading conduits. Diabetes is the condition that affects the parts of body such as eyes, kidneys, lungs, nervous system, heart and so on [4]. The prominent component of the human body is human eye, which deserves additional attention, as it impacts the vision.

DR is an eye disorder/contamination arising from diabetes, which is deferred and untreated. Diabetic-retinopathy has the aftereffects that initiate with curtailed micro-aneurysms that occur due to damaged blood vessels/nerves/ capillaries that are witnessed as red highlighting tiny specks (spherical in nature). When these retinal blood vein walls are broken, hemorrhages that are reddish in platelets appear [5]. Around the stage where the DR grows in intensity, strong exudates emerge in the eye that occurs due to the spillage of blood proteins and lipids that are yellowish in colour shading. After stronger development in the severity of the 'DR' infection, there is a lot of interference in the nerves that incites the structure of subtle exudates as white shading marks of cotton fleece in fact (gray in exudates of color) [6]. The Fig.1 illustrates a healthy retina.
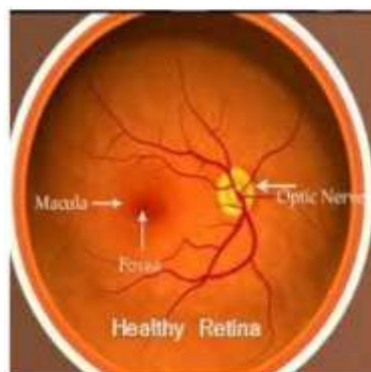
Figure 1: A Healthy Retina

In brief, diabetes is induced by a transition in the blood-vessel system of the human eye's possess. The retina layer at the back end of human eyes would be a transparent internal surface that is highly reliant on the light. The

damage is occurred by an increase of the glucose element of blood sugar levels that can injure veins / capillaries [7]. At the stage / crux where these veins-capillaries thicken-grow high, they will cause drops, that leads to loss of vision for the human eye. Pictorially, the 4 processes of DR & is displayed in the shape of a slide in the Fig 2, as well as described back to back as follows. The 4 DR classifications can be summed up as,

- Mild-Initial stage,
- Moderate-Mid way stage,
- Severe/non proliferative-pre final stage
- Proliferative-final stage.
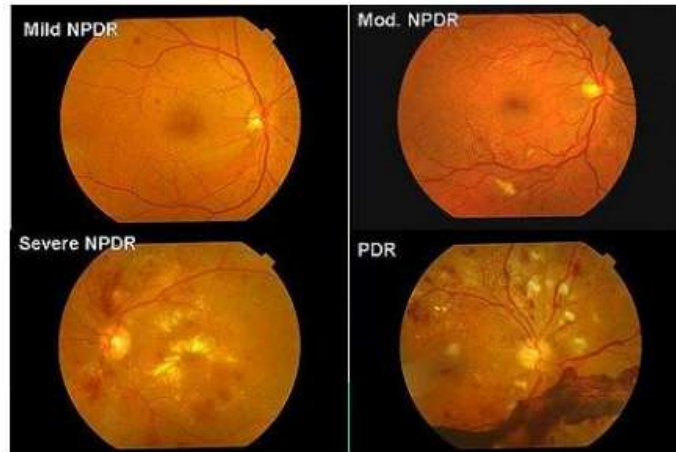
Figure 2: The four Chronic Stages of Diabetic Retinopathy

To deal with the first step, the moderate or the non-proliferated condition of DR, few portions of the veins or the blood capillaries placed beside the retina can swell in the form of a small bubble w.r.t. [8]. In this manner, the second stage, known as moderate / medium non-proliferative retinopathy, is affected by few retinal veins due to the rise in sugar levels, which results in blockage.

In the 3rd step, extreme or non-proliferative DR brings more clogged veins / capillaries with it, which causes much of the retina regions to never get adequate blood supply anymore, leading to more blockade in retina [9]. Hence, the human eye's retina could not grow further refurbished blood veins / capillaries that can be accustomed to repair weakened blood vessels with sufficient blood stream supply.

It will be the extreme stage of DR disorder in the 4th & final stage which is known as proliferative retinopathy. It is the driven process of the disorder, in which additional fresh blood vessels continue to grow in the retina, i.e. they continue to enlarge, but they may be quite fragile and irregular (minor in structure) [10]. They could spill blood in these lines (ooze out the blood) which would cause the lack of vision to reduce.

It required an immediate attention and to be taken care. If the condition arises, it must be attempted at an initial stage, or it will result to vision loss. Efficient DR therapies are there, but it helps only in the initial stage of diagnosis and constant tracking of diabetic sufferers.

DR treatment is conducted by retinal (fundus) imaging assessment. Physical grading of these photographs is really inefficient and resource consuming to assess the intensity of the DR. It appears as diabetes impacts the tiny blood vessels within the retina, the light-sensitive tissue, which is behind eye [11]. This smallest blood vessel can

trickle blood and fluid on the retina creates the causes like micro-aneurysms, hemorrhages, soft exudates, patches of cotton wool or venous loops. Sensing DR is a time draining and physical progress, which needs a qualified physician to review and analyze the digital colour fundus pictures of retina. Automatic diabetic retinopathy diagnosis would result in significant reduction in duration and energy. This field research suggested, a Deep Spectral Cluster Learning (DGW-DSCL) based on distributed Gaussian weight feature to diagnose the diabetic retinopathy to maximize the efficiency of the classifier.

The remaining of this research is structured as follows. Section 2 provides a depiction of similar research published in the recent article. Section 3 furnishes the suggested strategy and identification of diabetic Retinopathy by using classification method. Section 4 includes the performance evaluation of the proposed. Chapter 5, which contained the closing remarks.

II.   LITERATURE REVIEW

This segment addresses with a few of the current strategies that are employed with the assistance of machine learning systems to identify diabetic retinopathy.

Priya et al [12] have recommended three structures, such as Probabilistic Neural Network (PNN), Bayesian Vector Classification and Support Machine (SVM), to be represented and correlated with their outputs. Attributes including such blood vessels, NPDR image hemorrhages, and PDR image exudates are derived from the basic images utilizing image processing processes, and transmitted for categorization to the classifier.

Overall 350 fundus pictures were used, of which 100 were allocated for the purpose of practice, and 250 for research. Scrutiny outcomes reveals that PNN is 89.6% reliable, Bayes Classifier is 94.4% precise, while SVM holds the reliability of 97.6%.

Gandhi et al13] established the automated diagnosis of diabetic retinopathy by identifying exudates in images of colour fundus retinal and categorizes the severity of the abnormalities as well. SVM classifier made determination on the intensity level of the illness.

Gulshan et al [14] presented a deep learning approach to formulate an algorithm for automatic identification of diabetic retinopathy and diabetic macular edema in pictures of retinal fundus. This is a particular aspect of neural network configured for image recognition, termed a deep convolutional neural network, which was equipped by engaging the retrospective development data set that consist of 128175 retinal pictures, sorted 3 to 7 times for diabetic retinopathy, diabetic macular edema and image gradability by a certified ophthalmologist and senior citizens in ophthalmology. In this assessment of retinal fundus images from adults with diabetes, a deep-machine learning based algorithm had maximum sensitivity and precision for spotting traceable diabetic retinopathy.

Sopharak et al [15] proposed a list of researches on choice of functionality and categorization of exudates through classifiers of naive Bayes and support vector machine (SVM).

Then enable the naive Bayes model on a practicing set composed of 15 attributes derived from each of 1115867 exudate pixel examples, which is positive and a same amount of examples that is negative. Then executed the functionality on the naive Bayes method, withdrawing features from the classifier, one after the other periodically,

till the efficiency in classification ends up enhancing. Proceed to start with the best series of attribute from the naive Bayes classifier to locate the best SVM, and consistently incorporate the formerly excluded attributes to the classifier. Then balance the appropriate naive Bayes then SVM classifiers to a nearest neighbor (NN) classifier based on the series of attribute of both classifiers.

Bhatia et al [16] implemented a machine learning categorizing architectures that relies on characteristics derived from the results of various retinal image processing architectures, such as optic disk diameter, lesion specific (microaneurysms, exudates), image level (pre-screening, AM / FM, reliable evaluation). Conclusion were made to forecast the existence of diabetes retinopathy, with the help of alternating decision tree, AdaBoost, Naive Bayes, Random Forest and SVM.

Abràmoff et al [17] advanced a referable Diabetic Retinopathy (rDR), described as International Clinical Classification of Diabetic Retinopathy moderate, severe non proliferative (NPDR), proliferative DR, and/or Macular Edema (ME). For IDx-DR practice, neither Messidor-2 pictures nor the three retinal specialists defining the Messidor-2 reference criteria were being used. Sensitivity, accuracy, negative anticipating value, area under the curve (AUC) and their confidence intervals (CIs) were determined. Deep learning algorithms have the ability to increase DR screening performance and thereby avoid vision impairment and blindness from this debilitating disease.

Usher et al [18] suggested a method for automatically identifying characteristics of diabetic retinopathy in digital retinal colour pictures and testing their ability in diabetic retinopathy monitoring. In an internal-city diabetic retinopathy screening system, the Macular based 45 ° colour retinal photographs from 1273 patients.

To standardize colour and improve contrast, segregation to identify potential defects, and detection of wounds using an artificial neural network, a pre-processing method was utilized. The machine was equipped using a image sub-set of 500 patients and assessed by contrasting its efficiency with a human grader on a image test series of 773 patients.

Gargeya et al [19] built and tested a deep learning algorithm powered by data as a novel diagnostic method for automatic identification of DR. The algorithm analyzed photographs of colour fundus and marked them as sustainable (no retinopathy) or getting DR, recognizing appropriate medical reference scenarios. A sum of 75137 open access fundus photographs from diabetic sufferers were utilized to practice and assess an artificial intelligence algorithm to discern stable fundus from those with DR. The ground truth was assessed by a board of retinal experts for data set prior to performing an experiment. We validated this model even using the public MESSIDOR 2 and databases of E-ophtha for extrinsic validation.

Sopharak et al [20] suggested a series of optimally modified morphological operators to be used to track exudates on the non-dilated pupil and minimal-contrast pictures of patients with diabetic retinopathy. These dynamically observed exudates are confirmed as matched with the hand-drawn ground-truths of professional ophthalmologists. The tests are positive and the exudate identification sensitivity and specificity is 80% and 99.5% respectively.

Ting et al [21] developed a deep learning system (DLS) for the diagnosis of identifiable diabetic retinopathy, sight-cautionary diabetic retinopathy, possible glaucoma, and age-related macular degeneration (AMD) in society and medicine based across all indigenous people with diabetes. Through this process the efficiency of the DLS is examined as well.

Quellec et al [22] suggested a detector that was equipped to recognize referable DR, with pixel-level monitoring, surpasses modern algorithms equipped exclusively to identify such abnormalities. The suggested detector exceeds heatmap generation algorithms for ConvNets, at lesion point. This identifier is a portion of the Messidor system for Mobile Eye Pathology Scanning. As it does not base on qualified information or physical segregation to identify significant systems, the suggested conclusion is an innovative image mining process that enables to discover new biomarkers in pictures.

All these approaches executed supervised learning, where the fragmented image is contrasted with a reference picture. The major downside around is that it cannot test all of the attributes of the illness, but it contrasts only with the features of the picture being provided. So it is essential to identify DR procedures efficiently and accurately in this field.

III.   PROPOSED METHODOLOGY

This theoretical work suggests, Deep Spectral Cluster Learning (DGW-DSCL) relies on Distributed Gaussian Weight process to spot the Diabetic retinopathy in order to increase the efficiency of classifier. The suggested strategy includes two stages, known as, "preprocessing the pictures of fundus" and "the categorization for the identification of diabetic retinopathy illness". The suggested method begins its process by picking the image, as the further process relies on this step. The preferred images going through preprocessing in order to progress the contrast augmentation as well as removal of non-uniform illumination, which requires structural resemblance index for measuring the image purity, pursue by the fuzzy histogram equalization. The anticipated structure utilizes a fuzzy histogram equalization method in the stage of preprocessing the image is occupied in order to extending the quality of image as well evading or minimizing the non- uniform illumination on the image.

Here, the structural similarity index (SSI) metric is originally employed to assess the quality of the image. Then the equalization and advancement of comparison are achieved through the equalization of the novel Fuzzy histogram. Then patches of images are removed periodically from the preprocessed picture.

 And then the Deep Spectral Cluster Learning (DGW-DSCL) focused Distributed Gaussian Weight concept is implemented, which optimizes an embedding factor using a Gaussian weight function to combine the learned representations of identical entities into the same cluster, and contrasting entities to improve the effectiveness of spectral clustering. To addition enhance the consistency of the classification, it is suggested to predict their Diabetic Retinopathy (DR) probability by the improved deep patch level classifier, in which the classifier's weight values are amended by using the Improved Variability Iteration Ratio Grey Wolf (IVIR-GWO) algorithm. The common diabetic retinopathy diagnosis process is illustrated in Figure. 3.

Image Acquisition

fundus image preprocessing

Image Quality Assessment using Structural
Similarity Index (SSIM) Metric

Contrast Enhancement and illumination reduction
using novel fuzzy histogram equalization

Deep Spectral Clustering

Gaussian Weight Function Calculation

Eigenvalue Decomposition

Connection with Spectral Clustering

Detection of Diabetic Retinopathy (DR)

Estimation of Diabetic Retinopathy (DR) using
Enhanced Deep Patch-Level Classifier

Weights Optimization using Improved Variability
Iteration Ratio based grey wolf optimization (IVIR-
GWO) algorithm

Classified Result

Figure 3: General Process for the Detection of the Diabetic Retinopathy

3.1 Fundus Image Pre-processing

A. Image Quality Assessment using Structural Similarity Index Metric (SSI)

For image quality assessment, it is useful to apply the SSIM index locally rather than globally. At first, analytical characteristics of the picture are typically extremely spatially non-stationary [23].

Second, the distortions of the image, that might or might not rely on the stats of the local image, may also differ in space. Third, the human eye can perceive only a limited area in the image at a time with high-resolution, at normal optical ranges. Finally, certainty of regional quality can offer a spatially differing image quality chart that furnishes more information on the quality degradation of image and can be beneficial.

SSIM is being utilized to calculate similitude among two pictures and a complete reference measure. The calculation of image quality is focused on an original uncompressed or distortion-free image as a guide. The SSIM index measures the quality of a deformed image by analyzing the equivalence in light intensity, contrast, and composition, regionally within the reference and deformed image and by balancing these values over the whole

picture. Performance Assessment of Structural Similarity (SSIM) Index depends on the determination of three terms, that is to say, the luminance term, the contrast term, and the structural term.

The SSIM index assess a trial picture X in regard to an allusion picture Y to calibrate their optical relationship. SSIM figure out the eminence of X, as regards Y, by calibrating a local spatial index that is described as follows.

X and Y are the commensurate images (calibrated as patterns of pixels), and $x = \{x_i | i = 1,2, ..., N\}$ and $y = \{y_i | i = 1,2, ..., N\}$ are combination of windows of local square (calculated as sub-patterns of pixels) of X and Y, correspondingly; x and y are positioned at the exact spatial position in couple of pictures.

SSIM is represented with regard to the average pixel values, μ_x and μ_y, with pixel value standard deviations (SD) σ_x and σ_y at patches x and y and covariance (cross-correlation) σ_{xy} of x and y through the indications furnished below [24]:

$$l(x,y) = (2\mu_x\mu_y + C1)/(\mu_x^2 + \mu_y^2 + C1), \qquad (1)$$
$$c(x,y) = (2\sigma_x\sigma_y + C2)/(\sigma_x^2 + \sigma_y^2 + C2), \qquad (2)$$
$$r(x,y) = (\sigma_{xy} + C3)/(\sigma_x\sigma_y + C3), \qquad (3)$$

Where C1, C2, and C3 are parameters implemented to ignore imbalance, when $(\mu_x^2 + \mu_y^2)$, $(\sigma_x^2 + \sigma_y^2)$, or $\sigma_x\sigma_y$ nearing zero. The $l(x,y)$ index is associated with luminance variations, c(x,y) with dissimilarities in contrast, and r(x,y) with dissimilarities of structure among x and y. The most common structure of the SSIM index is describes as

$$SSIM(x,y) = [l(x,y)]^\alpha . [c(x,y)]^\beta . [r(x,y)]^\gamma \qquad (4)$$

Where α, β, and γ are criterions that represent the parallel priority of every element. SSIM(x, y) confines from 0 (entirely disparate) to 1 (similar patches). Finally, a mean SSIM index is determined to assess the worldwide affinity of picture.

B. *Augmentation of Contrast and Decreasing the Illumination Through Novel Fuzzy Histogram Equalization*

The received retinal images may differ in terms of image quality, illumination, and contrast, as it was derived from mass screening. The normalization of these variables tends to facilitate the equalization of the innovative fuzzy histogram. The suggested Fuzzy histogram equalization therefore not just to restores the brightness of the picture but still increases the nearby contrast of the primary image.

First of all, a fuzzy histogram is generated using fuzzy logic to help manage the inaccuracy values of the gray level, and it is divided into two sub histograms, focused on the original image's median value [24].

Then, every histogram is designated to a new set of dynamics. Ultimately, on every sub-histogram, the HE method is implemented autonomously. The FHE technique consists of the following operational stages:

(i) Fuzzification and enrichment of image;

(ii) Assessment of fuzzy histogram;

(iii) Segregating and equalizing histogram;

(iv) Defuzzification of image.

The following subdivisions contain the information about the procedures engaged.

(i) Fuzzification and Enrichment of Image

In picture fuzzification the depth of gray level is converted into a fuzzy plane with a value spanning from 0 to 1. An image f of size $M*N$ and level of intensity in the range $(0, L-1)$ be able to treated as a series of fuzzy individuals in the set notation of fuzzy, each with an associated process denoting the degree of having some gray level. The fuzzy pattern F matching to this image can be articulated in [24].

Any transitional value attributes to the status of utmost gray intensity of the pixel. A series containing of all μ_{ij} is known as the fuzzy property plane of the image. In favor of diminish the sum of image fuzziness, contrast enrichment is enforced to the fuzzy set F to create a further series of fuzzy, and the associated process of which is determined as,

$$\mu_F(i,j) = \begin{cases} 2*(\mu_{ij})^2 & 0 \le \mu_{ij} \le 0.5, \\ 1-(2*(1-\mu_{ij})^2) & 0.5 < \mu_{ij} \le 1. \end{cases} \quad (5)$$

(ii) Assessment of Fuzzy Histogram

We focus on the augmentation of contrast to improve the picture, which is obtained through adjusting the dark pixel into even darker and modifying the bright pixel even brighter. Therefore, fuzzy histogram is measured by means of (6) A fuzzy histogram is a sequence of original numbers $h(i)$, $i \in (0, 1 \ldots, L-1)$, here $h(i)$ is the existence regularity of gray levels that are over i. By treating the gray value (i, j) as a fuzzy number $_{(i,),}$ the fuzzy histogram is determined as

$$F \leftarrow h(i) + \sum_i \sum_j \mu_{F(i,j)}, (6)$$

Where $(i,)$ is the fuzzy associated process [24]. Statistical data of fuzzy can manage the inaccuracy of gray values even better than traditional crisp histograms, in this manner generating a smooth histogram.

(iii) Segregating and Equalizing Histogram

Rooted in, input median M, the fuzzy histogram F is decayed into two subhistograms F_L and F_U and the probability density process P_L and P_U of the sub histograms are explained in [24]. The corresponding accruing density operations for sub-histograms FL and FU are then described as,

$$C_L(F_k) = \sum_{j=0}^{m} P_L(F_j), (7)$$
$$C_U(F_k) = \sum_{j=m+1}^{L-1} P_U(F_j) \quad (8)$$

Let us describe the succeeding operations for transformation relying on accumulated density operation as,

$$T_L(F_k) = F_0 + (M - F_0)C_L(F_k), (9)$$
$$T_U(F_k) = M + 1 + (F_{L-1} - M + 1)C_U(F_k)(10)$$

The decayed sub-images are autonomously evened up on the basis of these conversion parameters, and the configuration of the resulting equalized sub-images that represent the output image. The yield image $g = \{(i,j)\}$ is articulated as,

$$g(i,j) = T_L(F_L) \cup T_U(F_U), (11)$$

Where,

$$T_L(F_L) = \{T_L(F(i,j)) | \forall F(i,j) \in F_L\}, \quad (12)$$
$$T_U(F_U) = \{T_U(F(i,j)) | \forall F(i,j) \in F_U\} \quad (13)$$

If we perceive that $0 \leq (F_k)$, $(F_k) \leq 1$, it is obvious to find that(F_L) equalizes the sub-image F_L over the range $(F_0,)$, whereas (F_U) equalizes the sub-image F_U over the range $(M+1, F_L-1)$. Resulting, the input image F is equalized up the complete dynamic range (F_0, F_{L-1}) with the limitation that the samples lower than the input median are assigned to (F_0, M) and the samples than the median are assigned to $(M+1, F_{L-1})$.

(iv) Defuzzification of Image

Defuzzification is the contrary of fuzzification. The algorithm traces the fuzzy plane back to intensities of gray level. Ultimately, the improved picture can be accessed by the following inversion:

$$G(i,j) = T^{-1}\big(g(i,j)\big) = \bigcup_{i=1}^{M} \bigcup_{j=1}^{N} g(i,j) * (L-1), \qquad (14)$$

Where (i, j) stands for the gray level of the $(i, j)^{th}$ pixel in the advanced image and $T-1$ denotes the inverse transformation of T. This method of brightness safeguarding, assures that the mean depth of the picture acquired post process is identical as that of the input.

3.2 Distributed Gaussian Weight Function based Deep Spectral Clustering(DGW-DSC)

Among all clustering algorithms, Spectral Clustering is prominent and extremely familiar. It functions by embedding the details in the Laplacian matrix's internal space, resulting from a couple of intelligent correspondence between data points, and employing k-means on this description to acquire the clusters. While spectral embedding of data metrics may be accomplished by a simple self-decomposition of their Laplacian graph matrix, the forthright calculation of eigenvectors with massive data series may be restrictive. In particular, it is equipped in a probabilistic manner that enables it to scale. Once equipped, this also provides a feature, enacted as a feed-forward network which assigns each input data speck to its spectral embedding coordinates. This chart can be enforced with ease to new test results. Deep learning is fed using restricted optimization, where the restriction (orthogonality of net outputs) is imposed by introducing a linear layer, the weights of which are dictated by the QR decomposition of their input. Furthermore, because good affinity functions are crucial to the success of spectral clustering, instead of using the standard embedding method and weight parameter to measure Gaussian affinity, deep networks can be equipped from unidentifiable data to recognize pair-wise distances and thus dramatically increase the quality of clustering.

To sum up, an outcome of clustering created by spectral clustering can be interpreted as executing eigenvalue decomposition on the graph Laplacian matrix extracted from a matrix of input data correlation. For most conventional spectral clustering algorithms, the resemblance calculation is essential because such algorithms usually proceed with the similarity matrix of a provided set of data. Nevertheless, it is challenging to pick an acceptable resemblance calculation in advance for a provided set of data. To overcome this issue, recommend a Deep Spectral Cluster Learning-based Distributed Gaussian Weighted algorithm, which begins with a Gaussian weight algorithm for further spectral clustering analysis.

- ### *Spectral Clustering*

The anticipated strategy has been represented in this section, which explains its primary factors and defines its association with spectral clustering [25]. Determine the subsequent standard clustering system: *Let X =*

$\{x_1, \ldots, x_n\} \subseteq \mathbb{R}^d$ designate a assortnet of unlabeled data points received through some unknown distribution D; given a objective count of clusters k and a distance measure within spots, the aimis to grasp a parallel measure within spots in X and use it to study a plan that allocates each of $x_1, \ldots, x_n$ to one of k potential clusters, thus the related points appear to be brought together into the same cluster.

In this process employed the Spectral Net, a neural network strategy for spectral clustering. Once equipped, SpectralNet figure out a map $F_\theta : \mathbb{R}^d \to \mathbb{R}^k$ and a cluster assignment operation$c : \mathbb{R}^k \to \{1, \ldots k\}$.It assigns each source point x to an output $y = F_\theta(x)$ and furnishes its cluster assignment $c(y)$. The spectral map F_θ is executed by a neural network, and the parameter vector θstands for the network weights.

- ***Learning the Spectral Map F_θ***

The primary learning process in SpectralNet, element is depicted. To this point, let $w : \mathbb{R}^d \times \mathbb{R}^d [0, \infty)$ be a symmetric similarity operation, such that $w(x, x')$articulated the resemblance within x and x'. Specified w, would like points x, x' which are comparable to each other (i.e., with large $w(x, x')$) to be embedded precise to each other. Hence, determine the loss

$$\mathcal{L}_{spectralNet}(\theta) = E[w(x, x')\|y - y'\|^2 \quad (15)$$

Where$y, y' \in \mathbb{R}^k$ the anticipation is captured towards couple of i.i.d. components(x, x') received from D, and θindicates the specifications of the map $y = F_\theta(x)$.Undoubtedly, the loss $\mathcal{L}_{spectralNet}(\theta)$ can bediminished by delineated entire points to the same output vector $(F_\theta(x) = y_0 \, for \, all \, x)$. To thwart this, need that the outputs will be orthonormal in anticipationin respect to D, i.e.,

$$E[yy^T] = I_{k \times k.} \quad (16)$$

As Distribution D is unclear, overwrite the anticipations in (16) and (17) by their experimental analogs. In fact, implement the optimization in a probabilistic manner. Particularly, at each iteration randomly sample a minibatch of msamples, which without hammering majority indication$x_1, \ldots, x_m \subseteq \chi$, and systematize them in an $m \times d$ matrix X whose ith row includes x_i^T. And then diminish the loss

$$\mathcal{L}_{spectralNet}(\theta) = \frac{1}{m^2} \sum_{i,j=1}^{m} W_{i,j} \left\| y_i - y_j' \right\|^2 \quad (17)$$

Where$y_i = F_\theta(x_i)$ and W is a $m \times m$ matrix such that $W_{i,j} = w(x_i, x_j)$.theanalogue of (18) for a small tiny batch is

$$\frac{1}{m} Y^T Y = I_{k \times k} \quad (18)$$

Where Y is a $m \times k$ matrix of the outputs whose ith row is y_i^T.

The map $F_\theta$has a usual neural network whose final layer implements the limitation on orthogonality. This layer receives input from k units, and performs as a linear layer with k results, where the weights are place to orthogonalize the output Y for the minibatch X. Let $\tilde{Y}$indicate the $m \times k$ matrix accommodating the inputs to this layer for X (i.e., the outputs of F_θ over the mini batch prior to orthogonalization), a linear map that orthogonalize the columns of $\tilde{Y}$ is evaluated via its QR decomposition.

When instructing this spectral map in a coordinate descent pattern, where substitute between orthogonalization and phases of the gradient. Both of these measures requires an individual mini-batch (maybe different sizes),

examined equally from the training series X. Using the QR decomposition in each orthogonalization stage, the weights of the final layer is regulated. Adjust the remaining weights in each stage of the gradient using normal back procreation. When SpectralNet is equipped, every weights are freezed (including those of the final layer), which functions literally as a linear layer. At Final, to achieve the cluster assignments $c_1, \ldots, c_n$ and procreate $x_1, \ldots, x_n$ through it to obtain the embeddings $y_1, \ldots, y_n \in \mathbb{R}^k$, and carry out k-means on them, attaining k cluster centers, as in regular spectral clustering.

The suggested deep spectral clustering approach on the basis of distributed Gaussian weight function comprises of two phases including computation of the Gaussian weight feature and decomposition of the own value. The definition of each stage in detail, will be expanded in the segment following. The reasoning underlying the recommended approach will also be offered when discussing the weighted operation of Distributed Gaussian.

- *Distributed Gaussian Weight Function Calculation*

The first step in the projected strategy is to establish the distance matrix from the provided sets of data and measure their respective Gaussian weight method on the basis of the data adaptive standard deviations. Let $x_1, \ldots, x_n$ be a set of n input data points inclusion of the d-dimensional space R^d. The arrangement of distance matrix $D \in R^{n \times n}$ is designated by $D_{p,q} = d(x_p, x_q)$ for $p \neq q$ and $D_{p,q} = 0$, where $d(x_p, x_q)$ symbolizes particular distance operation. The pair based distances can be calculated using any standard calculation of range. In this job, Euclidean distance is used as the calculation of distance. The measurement of data commutable standard deviations of the respective distances for each data point to the other data points is a critical factor in the computation of the Gaussian weight function. The Gaussian weight feature is extracted from the application of the Laplace operator with commutable standard deviation to the values in each row of distance matrix specified by,

$$L_{p,q} = \frac{1}{\sqrt{2\pi}\sigma_p^3}\left[1 - \frac{|x_p - x_q|^2}{\sigma_p^2}\right]\left[e^{-\frac{|x_p - x_q|^2}{2\pi\sigma_p^2}}\right] \qquad (19)$$

$$= \frac{1}{\sqrt{2\pi}\sigma_p^3}\left[1 - \frac{D_{p,q}^2}{\sigma_p^2}\right]\left[e^{-\frac{D_{p,q}^2}{\sigma_p^2}}\right] \qquad (20)$$

Where σ_p represents each row element standard deviation in a matrix D. A symmetric Gaussian weight function is one in which an alteration is accomplished to the Gaussian weight function which is given as $L_{p,q}^s = \frac{1}{2}(L_{p,q} + L_{q,p})$ for mutual correlation integration among data pairs. Gaussian weight function characteristics and properties does not get affected due to the alteration of the function. It is validated that Laplacian is a well-known operator suitable for image analysis for the purpose of boundary identification by utilizing zero-crossing of Laplacian which is a key factor for integrating the Gaussian weight function local cluster information for every data. The attainment of inter-cluster structure is another important factor in creating distance matrix which is established on Laplace operator with the estimated adaptive standard deviation. Here boundary is nothing but zero crossing location which is grouped under same cluster on estimation of each data point with the other ones and with the different cluster data points. The exposure of each data point with the other ones is accomplished by positive or negative G magnitudes for every data and the discrimination capability is raised by successful integration of Gaussian weight function.

Considering $Y = (y_1, y_2, ..., y_n)^T \in R^{1 \times n}$ notates the cluster relationship indicator and L notates the Gaussian weight function for expedition of distance-based spectral clustering investigation. The neighboring data points inner product is usually greater than zero due to the alike Gaussian weights to the further data points. The inner product distant data points is comparatively less than zero since there exist dissimilar signs for corresponding elements row vectors. The cluster relationship indicators between two arbitrary rows are as follows:

$$y_i y_j = \langle L_i, L_j \rangle = \begin{cases} > 0, & \text{where } y_i \text{ and } y_j \text{ beloing to the same cluster,} \\ \leq 0, & \text{where } y_i \text{ and } y_j \text{ beloing to the different cluster,} \end{cases} \quad (21)$$

Where L_i and L_j characterize the ith row and jth row in the Gaussian weight function, respectively, and <A, B> is the inner product of vectors A and B. The intra-cluster inner product of the weight relationships is maximized by optimal selection of input dataset bipartition and thereby maximizing the following objective function.

$$\sum_{i,j} y_i y_j L_{i,j} = \sum_i y_i \sum_j L_{i,j} y_j = Y^T L Y \quad (22)$$

As a result, the maximum Eigen value solution to the generalized Eigen value problem by $LY = \lambda Y$ is obtained from maximizing the objective function by the vector Y. The intra cluster inner product of pair wise relationships is maximized by optimization practice in which Gaussian weight function diagonalization is accomplished by the magnitude order of the eigenvector elements with the largest Eigen value.

- *Eigen value Decomposition*

The eigenvector with the largest Eigen value of the symmetric Gaussian weight function is chosen for intra-cluster inner product of pair wise relationships maximization which is the motivation for decomposition for Eigen value. Also the reordering of data points indices is done to other reordered weight function points which is nearby. The distance matrix D is reorganized by exploiting the largest eigenvalue, λ_1, of L^S in the eigenvector V_1. The order is well-defined by index permutation $\varphi(1, 2, ..., n) = (\varphi_1, \varphi_2, ..., \varphi_n)$ by letting the eigenvector $V_1 = (v_1^1, v_2^1, ..., v_n^1)^T$. The permutation vector can be represented as $\varphi(V_1) = (v_{\varphi 1}^1, v_{\varphi 2}^1, ..., v_{\varphi n}^1)^T$, where $v_{\varphi 1}^1 \leq v_{\varphi 2}^1 \leq \cdots \leq v_{\varphi n}^1$ for the eigenvector V_1. The representation of elemental reordered distance matrix R is given as $R_{\varphi_p, \varphi_q} = D_{p,q}$.

3.3 Estimation of Diabetic Retinopathy (DR) using Enhanced Deep Patch-Level Classifier

The DR lesions are initially identified before segregation of whole retinal image. The extraction of preprocessed image [26] is recurrently accomplished from Image patches. Their DR probabilities estimation is accomplished by providing into CNN-based patch-level classifier

Let X notates a preprocessed image with a size of $H \times W$ pixels. Let the sliding window size is described by $K \times K$ pixels and the stride be d pixels. X is then decomposed into a bag of image patches $\{c_{i,j}\}$, where $i \in \{1, 2, ..., \lceil (H - K)/d \rceil + 1\}$ and $j \in \{1, 2, ..., \lceil (W - K)/d \rceil + 1\}$ are the vertical and horizontal index, respectively. The patches' spatial information is stored by the indexes. On behalf of every patch $c_{i,j}$, the position of its top-left corner (h_i, w_j) is as trails:

$$h_i = \begin{cases} 1 + (i - 1) * d & if \ (i - 1) * d + K \leq H, \\ H - (K - 1) & otherwise, \end{cases} \quad (23)$$

And

$$w_j = \begin{cases} 1 + (j-1)*d & if\ (j-1)*d + K \leq W, \\ W - (K-1) & otherwise, \end{cases} \quad (24)$$

There involves various number of patches in every bag and CNN's input size is matched by resizing of the patches. The pre-trained AlexNet is greatly involved in revision of patch-level classifier and mis-selection of the DR images normal patches for training effects in the parameters vibration and a final breakdown of the training process is circumvented by adjusting the patches for DR detection.

The multiple functional layers are the key factors in attaining feature learning and image classification in the original AlexNet architecture. There are four layer groupings, namely the convolution layer, pooling layer, activation layer and auxiliary layer in the functional layers. Convolutional layer or a fully connected (FC) layer are present in the convolution layer. The approximation of any function for classification is accomplished by stack of FC layers which acts as a classifier. Following which is the pooling layer, in which pooling is realistic after the convolutional layer for enhancement of learned features translation invariance. The activation layers consist of rectified linear unit (ReLU) layers and a softmax layer. In particular the addition of convolution layers (except the last FC layer) aids in transformation of learned features non-linearly into more complex ones and the addition of softmax layer into the last FC layer maps its output into a probability distribution for all classes. The auxiliary layers consist of response normalisation (LRN) layers and dropout layers which helps in controlling the responses across feature channels which in turn enhances model's generalisation for image classification.

The last 1000-way FC layer with a two-way FC layer is substituted with the pre-trained AlexNet and re-initialization of its filter weights from a Gaussian distribution with standard deviation of 0.01 is accomplished for estimation of patch-level DR. T probability distribution $p(c_{i,j}) = [p_1(c_{i,j})\ p_2(c_{i,j})]^{\top}$ is obtained for each image patch by terminal softmax layer ci, j, where $p_1(c_{i,j})$ is the normal probability and $p_2(c_{i,j})$ is the DR probability.

- ***Optimization of Weights using Improved Variability Iteration Ratio based Grey Wolf Optimization (IVIR-GWO) Algorithm***

One among the novel heuristic swarm intelligent optimization algorithm is the grey wolf optimizer. The great ability of top predators wolf is to incarceration prey in the food chain. There persists a rigid social hierarchy [27] in wolves characteristics which is almost like social life. The wolves are classified into four types of wolf for internal leadership hierarchy. The best individual, second best individual and third best individual are verified as alpha, beta, and delta, and the rest of the individuals are deliberated as omega. The hunting in DWO is accomplished by guiding alpha, beta, and delta. They also assist other wolves (W)have a tendency to the finest area in searching space. The calculation of possible position of prey is attained by three wolves alpha, beta, and delta in iterative searching method. The updation of the locations of wolves in optimization process depends on Eqs (25) and (26).

$$\vec{D} = |\vec{C}.\vec{X}_p(t) - \vec{X}(t)| \quad (25)$$
$$\vec{X}(t+1) = \vec{X}_p(t) - \vec{A}.\vec{D} \quad (26)$$

Where, t symbolizes the t-th iteration, $\vec{A}$ and $\vec{C}$ are coefficient vector, $\vec{X}_p$ is the position vector of prey, $\vec{X}$ symbolizes the wolf position. The vector $\vec{A}$ and $\vec{C}$ can be articulated by

$$\vec{A} = 2a.\vec{r}_1 - \vec{a} \quad (27)$$

$$\vec{C} = 2.\vec{r}_2 \ (28)$$

Where, the coefficient $\vec{a}$ linearly drops from 2 to 0 with the rising of iteration number, $\vec{r}_1$ and $\vec{r}_2$ are random vector positioned in the scope [0, 1].
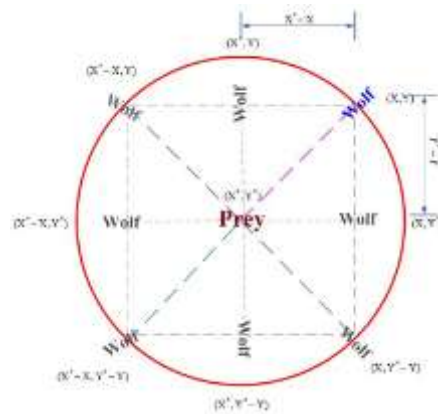
Figure 4: Position and Possible Location of Prey

Principle for the rules of position upgrading, defined in Eqs (25) and (26). It can be identified in Fig 4 The wolf at the location (X, Y) may move around the prey in compliance with the revised formulas above. Even if Fig 4 indicates only 7 positions to which the wolf has the chances to move, by modifying the random parameters C and A, the wolf can move to any location in the constant space close to the prey. In the GWO, it regularly considers that the alpha, beta, and delta positions are probably to be the prey (optimum) location. The best individual, second-best individual and third-best individual acquired as of now, are reported as alpha, beta, and delta in the iteration search method accordingly. Nevertheless, other wolves are regarded as omega, are change their positions as per alpha, beta, and delta ranges. The subsequent mathematical equations was used to modify the wolf omega's positions. The mathematical model which updates wolf's location is demonstrated in Fig. 5.
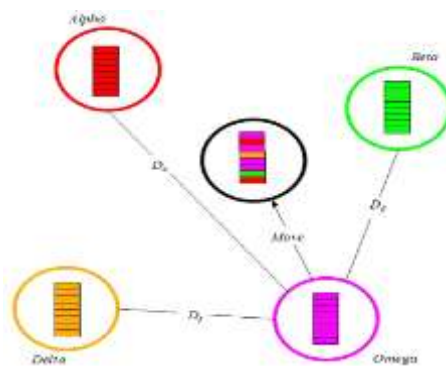
Figure 5: Position Updation of GWO

$$\vec{D}_\alpha = \left| \vec{C}_1.\vec{X}_\alpha - \vec{X} \right| \ (29)$$
$$\vec{D}_\beta = \left| \vec{C}_2.\vec{X}_\beta - \vec{X} \right| \ (30)$$
$$\vec{D}_\delta = \left| \vec{C}_3.\vec{X}_\delta - \vec{X} \right| \ (31)$$

where, $\vec{X}_\alpha$, $\vec{X}_\beta$ and $\vec{X}_\delta$ are the position vector of alpha, beta, and delta, respectively. $\vec{C}_1$, $\vec{C}_2$, $\vec{C}_3$ are randomly generated vectors, $\vec{X}$ represents the position vector of current individual. The Eqs (29), (30) and (31) respectively

calculate the distances between the position of current individual and that of individual alpha, beta, and delta. So the final position vectors of the current individual are calculated by:

$$\vec{X}_1 = \vec{X}_\alpha - \vec{A}_1.(\vec{D}_\alpha) \qquad (32)$$
$$\vec{X}_2 = \vec{X}_\beta - \vec{A}_2.(\vec{D}_\beta) \qquad (33)$$
$$\vec{X}_3 = \vec{X}_\delta - \vec{A}_3.(\vec{D}_\delta)(34)$$
$$\vec{X}(t+1) = \frac{\vec{X}_1 + \vec{X}_2 + \vec{X}_3}{3} \qquad (35)$$

Where, $\vec{A}_1$, $\vec{A}_2$, $\vec{A}_3$ are randomly generated vectors, and t represents the number of iterations. In the plane, three points is able to determine a region. Thus, the scope of position of the prey can be determined by the best three wolves.

- *Improved Variability Iteration Ratio based Grey Wolf Optimization*

The GWO, whose objective remedy is evaluated extensively using three approaches, will substantially reduce the risk of falling into the local intense From the aforementioned formula, it can be displayed that Eqs (29–31) determines the step scale of the omega towards alpha, beta, and delta, accordingly. Eqs (38–41) determines the finishing positions of the omega wolves. The ability to discover and manipulation have significant impact on an algorithm's search results. For the GWO, discovery refers to a wolf leave the initial quest route in a certain range and searching for a new direction that represents the potential of the wolf to explore unfamiliar areas. Manipulation refers to the fact that in a certain way a wolf proceeds to look more closely on the initial course, and will mean that the wolf completes a thorough analysis of the area that has been examined. It can be observed that the two random and adaptive vectors $\vec{A}$ and $\vec{C}$ can be utilized to attain an appropriate negotiation between ability to discover and manipulation of the GWO. As is exposed in Fig. 6, when $\vec{A}$ is bigger than 1 and is less than −1, that is $\vec{A} > 1$, the wolf reveals ability to discover. When the value of vector $\vec{C}$ is higher than 1, it can also augment the wolf's ability to discover. In contrast, when $\vec{A} < 1$ and Cwolf's capacity of manipulation is advanced. For escalating the wolf's capacity of manipulation gradually, the vector $\vec{A}$ decreases linearly with the iterations number rising. Nevertheless, in the course of optimization the value of $\vec{C}$ is created randomly, that could move discovery and manipulation of the wolf arrive at an equilibrium at any phase. In particular in the final phases of the iteration, it can stop locking the algorithm into a localintense.
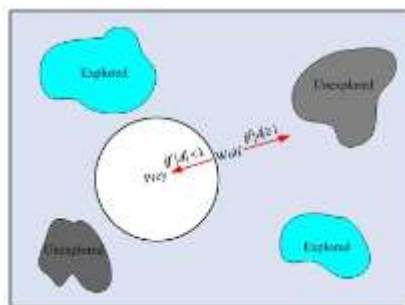
Figure 6: Exploration and Exploitation Search of GWO

The GWO has a high potential for discovery and can preclude the algorithm from slipping into the optimal locale. For the GWO, the appropriate balance between discovery capacity and manipulation skill is very easy to reach, such that other difficult issues can be resolved efficiently.

An optimization algorithm's primary objective is to reach a global optimum. It has to attain two steps in this operation, that is to say, discovery and manipulation.i Discovery deals with dispersion of the search operators all over the search range, accompanied by converging in the extraction process to a global optimum. Appropriate equilibrium between discovery and manipulation needs to be established to reach global optimum convergence while minimizing local minima. Therefore, more sophisticated algorithms are often required to tackle numerous optimization issues.

The GWO algorithm explains the statistical model illustrating the hunting nature and social structure of gray wolfs. Discovery and manipulation at GWO relies on two criteria: $\vec{v}$ and $\overrightarrow{A}$. Half of the iterations are loyal to the process of discovery, i.e., when $\vec{A} \geq 1$ and the remaining half are allocated to the process of manipulation, i.e., when $\vec{A} < 1$. Maximum discovery leads to reduced risk of instability at the optimal locale. The changes was performed with the proportion of discovery and manipulation to be preserved in mind. The IGWO expands the potential of discovery by rising parameter nonlinearity $\vec{A}$ as presented below:

$$v = 2\left(1 - \frac{t^i}{T^i}\right) \quad (36)$$

Where the existing variability iteration ratio is t and the highest number of iterations is T. The difference of $\vec{v}$ over the course of 500 iterations for contrast values of i which assists in deciding the value of i (i= 3) to some extent escalating the quantity of iterations designated for discovery. The variation of $\vec{A}$ as a consequence of variation in $\vec{v}$ using box plot. In addition altering the value of $\vec{v}$, in terms of additionaldevelop the ability of discovery, the method to revise the point is altered by adding minor randomness in the position revise of search operators. Here, a approach of measuring the vectors $\overrightarrow{D_a'}$, $\overrightarrow{D_b'}$, and $\overrightarrow{D_c'}$ is enforced to keep the trapping away from optimal locale. The strategy of the updated positions is as follows:

$$\overrightarrow{D_a} = |\vec{C_1}\vec{X}_{ra} - \vec{X}_{rb}|, \overrightarrow{D_b} = |\vec{C_2}\vec{X}_{rb} - \vec{X}_{rd}|, \overrightarrow{D_d} = |\vec{C_3}\vec{X}_{rd} - \vec{X}_{ra}| \quad (37)$$

$$\vec{X}_1' = |\overrightarrow{X_a} - \overrightarrow{A_1}.\,(\overrightarrow{D_a'})|, \quad (38)$$

$$\vec{X}_2' = |\overrightarrow{X_b} - \overrightarrow{A_2}.\,(\overrightarrow{D_b'})|, \quad (39)$$

$$\vec{X}_3' = |\overrightarrow{X_d} - \overrightarrow{A_3}.\,(\overrightarrow{D_d'})|, \quad (40)$$

$$\vec{X}'(t+1) = \frac{(\overrightarrow{X_1'} + \vec{X}_2' + \vec{X}_3')}{3} \quad (41)$$

Where ra, rb, and rd are random search operators from within the population such that $ra \neq rb \neq rd$. The vectors $\overrightarrow{D_a'}$, $\overrightarrow{D_b'}$, and $\overrightarrow{D_c'}$ are used only when the value of A is higher than 1.

IV. RESULTS AND DISCUSSION

The dataset of DIARETDB1 consists of 89 retinal images with an exclusive resolution of 1500 x 1152 pixels. Instead of using DR grading, four professionals were asked to identify the sites of DR lesions, including micro

aneurysms, hemorrhages, hard exudates and cotton-wool spots. Average map of confidence of each category of lesion is then issued for each picture [27].

Accuracy is calculated as the ratio of properly found positive findings to all the positive observations anticipated [28].

$$Precision = TP/TP+FP \qquad (42)$$

Sensitivity is described in as the ratio of appropriately recognized positive observations to total observations [29].

$$Recall = TP/TP+FN \qquad (43)$$

F1 value is calculated as the weighted average of certainty and Recall [29]. As a consequence, it absorbs false positive as well as false negatives.

$$F1\ Score = 2*(Recall * Precision) / (Recall + Precision) \quad (44)$$

$$Accuracy = (TP+FP)/(TP+TN+FP+FN) \qquad (45)$$

The precision is measured as follows in terms of the positive and negative:

Table 1: Result of Efficiency Analysis between the Suggested Methods and Existing Methods

Metrics	CNN	TPCNN	DMIL	EDCNN	DGW-DSCL
Precision	53.90	55.23	58.23	61.57	66.89
Recall	82.73	86.36	91.64	93.98	96.51
F-measure	65.27	67.37	71.21	74.39	79.01
Accuracy	82.59	86.62	91.37	94.19	96.46

Table 1. shows the Tabulates the proposed and existing detection of diabetic retinopathy techniques
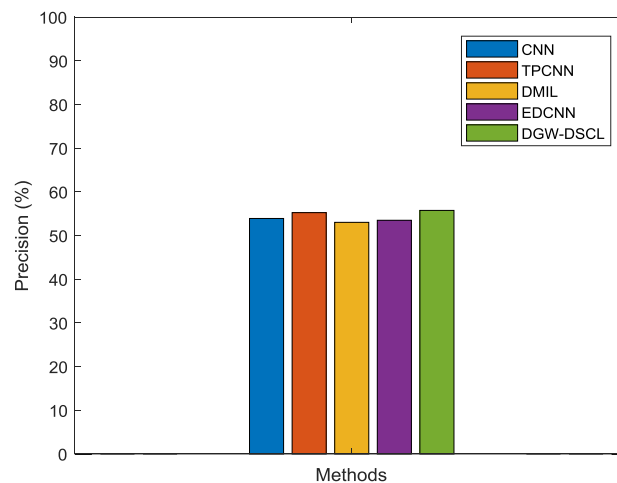
Figure 7: Precision Comparison of the Proposed DGW-DSCL

It is being observed that better precision is achieved by the recommended DGW-DSCL process as compared with current strategies. The resulting images produced by the proposed Fuzzy histogram equalization process are promising, and this preprocessing approach improves the DR detection method's achievement level. From figure 7, we can observe that, the precision level of the proposed DGW-DSCL process is 66.89 percent, while the metric of EDCNN method is 61.57 percent and the metric of DMIL method is 58.23 percent and the metric of TPCNN method is 55.23 percent.
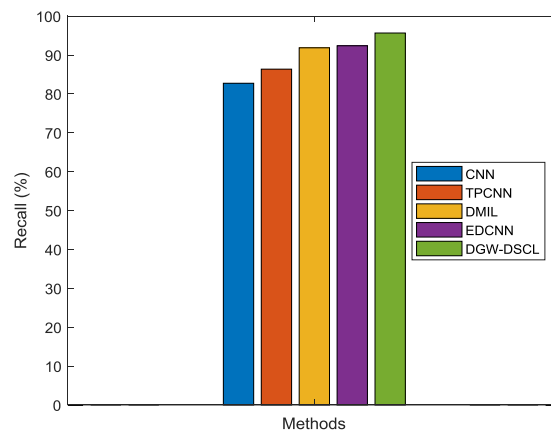
Figure 8: Recall Comparison of the Proposed DGW-DSCL

Within Fig.8.displays recall comparison of the suggested DGW-DSCL is promising with contrast to current techniques. The suggested DGW-DSCL achieves 96.51% which is greater recall performance, while the metric of the EDCNN process is 93.98%, the metric of the DMIL process is 91.64% and the metric of the TPCNN process is 86.36%. It can be said that, at the initiation of the practice, the recall increases quickly and maintains the performance by decreasing the range within the points using Structural Similarity Metrics (SSI).
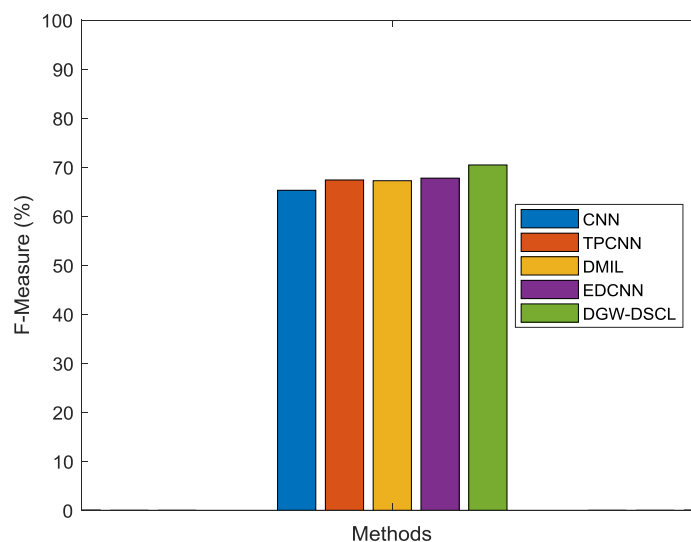
Figure 9: F-Measure Comparison of the Proposed DGW-DSCL

Fig.9 demonstrates the F-measure analysis of the suggested IVIR-GWO is efficient as contrasted to the current strategies. At first, adding Heterogeneity Iteration Ratio will maximize the diversity of wolves, i.e. increase the complexity of the solution such that the algorithm leaps out the local intense. Secondly, the selection approach enables the algorithm good discovery capabilities in the early search process and has better ability of discovery in the later search process, thereby, both accuracy of search and velocity of convergence are enhanced.
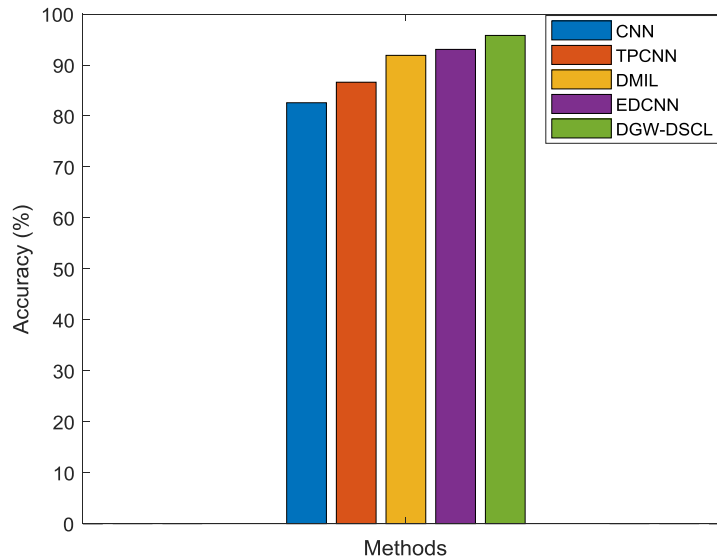
Figure 10: Accuracy Comparison of the Proposed DGW-DSCL

The efficiency of the suggested approach is improved by computing the Spectral clustering on the basis of distributed Gaussian weight function, where the calculation of the adaptive standard deviations of the respective distances for each data point is effectively optimized. From Fig.10. Displays a higher performance ratio with the DGW-DSCL suggested as compared to current approaches. The suggested DGW-DSCL results in a higher precision of 96.46% while the metric of the EDCNN method is 94.19%, the metric of the DMIL method is 91.37% and the metric of the TPCNN method is 86.62%.

V. CONCLUSION

Diabetic retinopathy is the very severe diabetes condition that can result in legal impairment, which is a significant public health issue. The proposed theoretical work allows for an automatic diabetic retinopathy identification system. In the preprocessing phase, the proposed method used a variety of blurry strategies to improve the image clarity and to prevent or decrease the non-uniform illumination of the images. Recently implemented is the Deep Spectral Cluster Learning (DGW-DSCL) based Distributed Gaussian Weight method, which optimizes an embedding feature to measure distances, and scientifically demonstrates that this results in improved output. From this, deep spectral clustering convergence with deep learning offers a valuable method for unmonitored deep learning. In addition to providing an upgraded deep patch-level classifier, weight values of the classifier are optimized through Improved Variability Iteration Ratio based Grey Wolf Optimization (IVIR-GWO) algorithm. The proposed IVIR-GWO provides the correct balance between discovery and manipulation, which accelerates

integration and improves GWO's optimization performance. The suggested improved classifier of deep patch level model forecasts the class label for DR, thus evaluating 96.46 percent precision. The new program is also useful for physicians who treat DR to prescribe the care of the affected sufferer and to prevent vision impairment. Future research contains strengthening the proposed approach by manipulating the outcomes of which the Deep Spectral learning system is taken into account instead of using a regular probabilistic gradient descent solver.

REFERENCES

[1] Gupta, S., &Karandikar, A. M. (2015). Diagnosis of diabetic retinopathy using machine learning. *Journal of Research and Development*, *3*(2), 1-6.

[2] Kumaran, Y., &Patil, C. M. A Brief Review of the Detection of Diabetic Retinopathy in Human Eyes Using Pre-Processing & Segmentation Techniques.

[3] Gupta, S., &Karandikar, A. M. (2015). Diagnosis of diabetic retinopathy using machine learning. *Journal of Research and Development*, *3*(2), 1-6.

[4] Mankar, B. S., & Rout, N. (2016). Automatic detection of diabetic retinopathy using morphological operation and machine learning. *ABHIYANTRIKI Int. J. Eng. Technol*, *3*(5), 12-19.

[5] Lachure, J., Deorankar, A. V., Lachure, S., Gupta, S., &Jadhav, R. (2015, June). Diabetic Retinopathy using morphological operations and machine learning. In *2015 IEEE International Advance Computing Conference (IACC)* (pp. 617-622). IEEE.

[6] Islam, M., Dinh, A. V., & Wahid, K. A. (2017). Automated diabetic retinopathy detection using bag of words approach. *Journal of Biomedical Science and Engineering*, *10*(05), 86.

[7] Somasundaram, A., &Prabhu, J. (2013). Detection of exudates for the diagnosis of diabetic retinopathy. *International Journal of Innovation and Applied Studies*, *3*(1), 116-120.

[8] Vimala, G. A. G., &Mohideen, S. K. (2012). An efficient approach for detection of exudates in diabetic retinopathy images using clustering algorithm. *IOSR Journal of Computer Engineering (IOSRJCE)*, *2*, 43-48.

[9] Shanthi, T., &Sabeenian, R. S. (2019). Modified Alexnet architecture for classification of diabetic retinopathy images. *Computers & Electrical Engineering*, *76*, 56-64.

[10] Mankar, B. S., & Rout, N. (2016). Automatic detection of diabetic retinopathy using morphological operation and machine learning. *ABHIYANTRIKI Int. J. Eng. Technol*, *3*(5), 12-19.

[11] Savu, M., Popescu, D., &Ichim, L. (2017, October). Blood vessel segmentation in eye fundus images. In *2017 International Conference on Smart Systems and Technologies (SST)* (pp. 245-249). IEEE.

[12] Priya, R., &Aruna, P. (2013). Diagnosis of diabetic retinopathy using machine learning techniques. *ICTACT Journal on soft computing*, *3*(4), 563-575.

[13] Gandhi, M., &Dhanasekaran, R. (2013, April). Diagnosis of diabetic retinopathy using morphological process and SVM classifier. In *2013 International Conference on Communication and Signal Processing* (pp. 873-877). IEEE.

[14] Gulshan, V., Peng, L., Coram, M., Stumpe, M. C., Wu, D., Narayanaswamy, A., & Kim, R. (2016). Development and validation of a deep learning algorithm for detection of diabetic retinopathy in retinal fundus photographs. *Jama*, *316*(22), 2402-2410.

[15] Sopharak, A., Dailey, M. N., Uyyanonvara, B., Barman, S., Williamson, T., Nwe, K. T., & Moe, Y. A. (2010). Machine learning approach to automatic exudate detection in retinal images from diabetic patients. *Journal of Modern optics*, *57*(2), 124-135.

[16] Bhatia, K., Arora, S., &Tomar, R. (2016, October). Diagnosis of diabetic retinopathy using machine learning classification algorithm. In *2016 2nd International Conference on Next Generation Computing Technologies (NGCT)* (pp. 347-351). IEEE.

[17] Abràmoff, M. D., Lou, Y., Erginay, A., Clarida, W., Amelon, R., Folk, J. C., &Niemeijer, M. (2016). Improved automated detection of diabetic retinopathy on a publicly available dataset through integration of deep learning. *Investigative ophthalmology & visual science*, *57*(13), 5200-5206.

[18] Usher, D., Dumskyj, M., Himaga, M., Williamson, T. H., Nussey, S., & Boyce, J. (2004). Automated detection of diabetic retinopathy in digital retinal images: a tool for diabetic retinopathy screening. *Diabetic Medicine*, *21*(1), 84-90.

[19] Gargeya, R., &Leng, T. (2017). Automated identification of diabetic retinopathy using deep learning. *Ophthalmology*, *124*(7), 962-969.

[20] Sopharak, A., Uyyanonvara, B., Barman, S., & Williamson, T. H. (2008). Automatic detection of diabetic retinopathy exudates from non-dilated retinal images using mathematical morphology methods. *Computerized medical imaging and graphics*, *32*(8), 720-727.

[21] Ting, D. S. W., Cheung, C. Y. L., Lim, G., Tan, G. S. W., Quang, N. D., Gan, A., ... & Wong, E. Y. M. (2017). Development and validation of a deep learning system for diabetic retinopathy and related eye diseases using retinal images from multiethnic populations with diabetes. *Jama*, *318*(22), 2211-2223.

[22] Quellec, G., Charrière, K., Boudi, Y., Cochener, B., &Lamard, M. (2017). Deep image mining for diabetic retinopathy screening. *Medical image analysis*, *39*, 178-193.

[23] Renieblas, G. P., Nogués, A. T., González, A. M., León, N. G., &del Castillo, E. G. (2017). Structural similarity index family for image quality assessment in radiological images. *Journal of Medical Imaging*, *4*(3), 035501.

[24] Usha Nandhini, & Lakshmi Prabha, S. Novel Fuzzy Pixel Value Stretching and Enhanced Deep Instance Learning for Detection of Diabetic Retinopathy, *Jour of Adv Research in Dynamical & Control Systems*, *pp. 494-505,Vol. 11, 10-Special Issue,* 2019.

[25] Zelnik-Manor, L., &Perona, P. (2005). Self-tuning spectral clustering. In *Advances in neural information processing systems* (pp. 1601-1608).

[26] Zhou, L., Zhao, Y., Yang, J., Yu, Q., & Xu, X. (2017). Deep multiple instance learning for automatic detection of diabetic retinopathy in retinal images. *IET Image Processing*, *12*(4), 563-571.

[27] El-Gaafary, A. A., Mohamed, Y. S., Hemeida, A. M., & Mohamed, A. A. A. (2015). Grey wolf optimization for multi input multi output system. *Universal Journal of Communications and Network*, *3*(1), 1-6.

[28] Soliman, O. S., & AboElhamd, E. (2014). Classification of diabetes mellitus using modified particle swarm optimization and least squares support vector machine. *arXiv preprint arXiv:1405.0549*.

[29] Powers, D.M., 2011. Evaluation: from precision, recall and F-measure to ROC, informedness, markedness and correlation. *Journal of Machine Learning Technologies* Vol. 2, no. 1, 2011, pp-37-63.